



Published in final edited form as:

Nature. ; 475(7354): 118–121. doi:10.1038/nature10126.

The Ribosome Uses Two Active Mechanisms to Unwind mRNA During Translation

Xiaohui Qu^{1,2}, Jin-Der Wen^{1,2,#}, Laura Lancaster³, Harry F. Noller³, Carlos Bustamante^{1,2,4,*}, and Ignacio Tinoco Jr.^{2,*}

¹Jason L. Choy Laboratory of Single Molecule Biophysics and QB3 Institute, University of California, Berkeley, California 94720, USA

²Department of Chemistry, University of California, Berkeley, California 94720, USA

³Department of Molecular and Cell, and Developmental Biology, and Center for Molecular Biology of RNA, University of California, Santa Cruz, California 95064, USA

⁴Department of Molecular and Cellular Biology, Department of Physics, and Howard Hughes Medical Institute, University of California, Berkeley, California 94720, USA

Abstract

The ribosome translates the genetic information encoded in messenger RNA into protein. Folded structures in the coding region of an mRNA represent a kinetic barrier that slows the peptide elongation rate, as the ribosome must disrupt structures it encounters in the mRNA at its entry site to enable translocation to the next codon. Such structures are exploited by the cell to create diverse strategies for translation regulation, such as programmed frameshifting^{1,2}, protein expression levels^{3,4}, ribosome localization⁵, and cotranslational protein folding⁶. Although strand separation activity is inherent to the ribosome, requiring no exogenous helicases⁷, its mechanism is still unknown. Here, using a single-molecule optical tweezers assay on mRNA hairpins, we find that the translation rate of identical codons at the decoding center is greatly influenced by the G•C content of folded structures at the mRNA entry site. Furthermore, force applied to the ends of the hairpin to favor its unfolding significantly speeds translation. Quantitative analysis of the force dependence of its helicase activity reveals that the ribosome, unlike previously studied helicases, uses two distinct active mechanisms to unwind mRNA structure: (i) it destabilizes the helical junction at the mRNA entry site by biasing its thermal fluctuations toward the open state, increasing the probability for the ribosome to translocate unhindered; and (ii) it also mechanically pulls apart the mRNA single-strands of the closed junction during the conformational changes that accompany ribosome translocation. Our results establish a quantitative mechanical basis for

Users may view, print, copy, download and text and data- mine the content in such documents, for the purposes of academic research, subject always to the full Conditions of use: http://www.nature.com/authors/editorial_policies/license.html#terms

Correspondence and requests for materials should be addressed to I.T. (intinoco@lbl.gov) or C.B. (carlos@alice.berkeley.edu).

[#]Present address: Institute of Molecular and Cellular Biology, National Taiwan University, Taipei 10617, Taiwan.

Supplementary Information is linked to the online version of the paper at www.nature.com/nature.

Author Contributions X.Q. and J.D.W. conducted the experiments and performed the analysis; X.Q., J.D.W. and L.L. prepared and provided experimental materials; and X.Q., J.D.W., L.L., H.F.N., C.B., and I.T. wrote the paper.

The authors declare no competing financial interests.

understanding the mechanism of regulation of the elongation rate of translation by structured mRNAs.

To monitor ribosome translation and mRNA unwinding with optical tweezers, we use a hairpin-forming mRNA that has a single-stranded 5' overhang that includes the Shine-Dalgarno sequence and the start codon for ribosome loading⁸ (Figures 1a and S1). Translation starts with the introduction of a translation mixture in the tweezers flow chamber.

Single-stranded mRNA enters the ribosome through the ring-shaped mRNA entry site formed by ribosomal proteins S3, S4 and S5, and wraps around the neck of the 30S ribosomal subunit in an RNA-rich channel that accommodates about 30 nucleotides⁹. The average tunnel diameter is smaller than that of an RNA double helix, so secondary structures in the mRNA must be disrupted for it to move through the tunnel. A crystal structure⁹, bulk oligonucleotide displacement assays⁷, and optical tweezers measurements reported here (Figure S2) yielded a distance of 13 ± 2 (s.d.) nucleotides from the first nucleotide in the P site to the mRNA entry site. Therefore, as shown in Figure 2a, when the ribosome translates codon *i* at the A site, translocation to the next codon requires the unwinding of codon (*i* + 4) downstream.

To investigate the effect of hairpin stability on the rate of translation, we designed two hairpin-containing mRNAs, hpVal_{GC50} and hpVal_{GC100}, that differ only in the hairpin region, specifically in the G•C content of the codons downstream of 10 Val codons (Figures 2a and S1). Translation of the third to tenth Val codons on hpVal_{GC50} mRNA is accompanied by unwinding of a helix with close to 50% G•C content (46%). For hpVal_{GC100} mRNA, translation of the third to sixth Val codons results in unwinding of the seventh to tenth Val codons, also forming a helix with similar G•C content (42%), but translation of the seventh to tenth Val codons is accompanied by unwinding the first four codons (Arg or Ala) that follow the Val stretch, a helix with 100% G•C content. Translation steps preceding the third Val codon were excluded from data analysis because the finite mixing time in the flow chamber made rate measurements for these first codons difficult. Unless noted otherwise, elongation factors were used at saturation concentrations (Figure S3) so that their binding to the ribosome was not rate limiting. Under our conditions, less than 5% of the ribosomes stalled before translating all the Val codons in the hpVal_{GC50} mRNA.

To characterize helicase activity, we apply different constant forces to the ends of these hairpins. Figure 1b shows a typical translation trajectory revealing periods of constant mRNA end-to-end distance (pauses) followed by periods of sudden distance increase (bursts). The burst between two pauses represents ribosome translocation, the movement of the ribosome from one codon to the next. We obtain single-codon resolution at forces above 11 pN; the upper force value accessible to these experiments is approximately 3 pN below the opening force (F_c) for the hairpin. When held at constant forces closer to F_c , the hairpin unfolds spontaneously before translation is finished. To extend this range and to measure the average translation rate for each individual ribosome down to 3 pN, we use a novel “force-drop/force-jump” technique (Figure S4).

Burst times (Figure S5) have an average duration of 22 ± 3 (s.e.m.) ms, and show no dependence on force or on the concentrations of elongation factors. Translation rates, which are determined by the pause lengths, depend monotonically on force (Figure 2b)—under saturating elongation factor concentrations the average pause time varies between ~ 2 s and ~ 4 s at high and low forces, respectively—and follow a Michaelis-Menten dependence on the concentrations of elongation factors EF-G and EF-Tu (Figure S3). These observations suggest that translocation can be considered as a single-barrier crossing process (see section 1 in supplementary discussion). A mechano-chemical analysis¹⁰ of the dependence of the translation rate on elongation factor concentration at high and low force was done to determine which kinetic steps in the reaction are affected by the application of force on the junction, and thus which kinetic steps involve motion of the ribosome through the junction. This analysis (see section 2 in supplementary discussion) showed that while K_m and V_{max} for both elongation factors increase with increasing force applied to the hairpin, their ratio is invariant. This invariance indicates that force does not affect the binding steps of these factors. Therefore, the translocation step, which does depend on force, can be separated from the previous biochemical steps (Scheme 1).

The translation rates for both hpVal_{GC50} mRNA ($\sim 50\%$ G•C unwinding) and hpVal_{GC100} mRNA (100% G•C unwinding) show a sigmoid dependence on force (Figure 2b). Clearly, the secondary structure of the mRNA represents a rate-limiting barrier to translation by the ribosome. The low-force plateau provides an estimate of the translation rate on double-stranded mRNA; the high-force plateau provides an estimate of the translation rate on single-stranded mRNA. The identical unwinding rates at the high-force plateaus for both 100% G•C and 50% G•C content indicate that single-strand rates are not significantly affected by the downstream sequences. The force, F_M , at the midpoint of the sigmoid transition between double-strand and single-strand rates increases with increasing G•C content, consistent with the greater thermodynamic stability of G•C-rich double strands. As expected, the average translation rates of unwinding the $\sim 50\%$ G•C region of hpVal_{GC100} mRNA and of winding the hpVal_{GC50} mRNA agree at all forces within experimental error (Figure S6).

Various qualitative unwinding models, such as a strand exclusion mechanism and a helix-destabilizing mechanism¹¹, have been proposed for processive helicases based on their structures. Mechanical studies of the unwinding activity of several nucleic acid helicases¹²⁻¹⁴, and HIV-1 reverse transcriptase (RT) on DNA templates¹⁵ have been interpreted in terms of the quantitative Betterton model^{12,16}. The junction at the end of a double strand fluctuates rapidly between open and closed states due to thermal energy. The Betterton model postulates that: (i) a helicase translocates through the open state of the junction; and (ii) an active helicase lowers the free energy of the open state relative to the closed state of the junction by the amount $-G_d$, thus biasing junction thermal fluctuations toward the open conformation. In a totally active helicase, $-G_d$ is much greater than the base pair free energy, so the junction is always open and no longer hinders translocation. A passive helicase ($-G_d = 0$) depends on junction opening by thermal fluctuations to translocate. Of course, in general a helicase will show an unwinding activity between the two extremes.

Applying the Betterton model to determine the extent of destabilization, G_d , of a helicase can be ambiguous when the step size is unknown and when back tracking can occur¹⁴. However, in our experiments, a three-base-pair step size is directly measured, and ribosome reverse translocation is not observed. Thus, our data and these two constraints are sufficient to rule out the Betterton model, as no combination of parameters in that model can fit simultaneously the observed low-force plateau, high-force plateau, and mid-point force F_M of the ribosomal helicase (Figure 2b). Clearly, additional interactions need to be incorporated to model the mRNA unwinding by a translating ribosome.

In the Betterton model the value of G_d that fits the mid-point force predicts a low-force plateau of nearly zero rate (Fig. 2b dashed black line), much smaller than we observe. This indicates that in addition to biasing the junction thermal breathing, the ribosome has an active mechanism to directly break open a closed junction during translocation. A minimal kinetic mechanism required by our results is the following:

Here all biochemical steps in a translation cycle^{17,18} other than the actual translocation step are condensed into a single irreversible rate constant, k_{peptide} , whereas $k_{\text{translocation}}^{ss}$ and $k_{\text{translocation}}^{ds}$ are the rates of translocation through an open (single-stranded) and closed (double-stranded) junction, respectively. In this scheme, k_{open} and k_{closed} depend on force, junction G•C content, and G_d ; $k_{\text{translocation}}^{ds}$ only depends on junction G•C content; $k_{\text{translocation}}^{ss}$ is independent of these three factors. Setting $k_{\text{translocation}}^{ds} = 0$ reduces this kinetic mechanism to the Betterton model.

The kinetics equation derived from the mechanism of Scheme 1 is given by (see section 3 in supplementary discussion):

$$v(F) = v_{ss} \cdot f_{\text{open}}(F) + v_{ds} \cdot (1 - f_{\text{open}}(F)) \quad (1)$$

where

$$\begin{aligned} v_{ss} &= k_{\text{translocation}}^{ss} / (1 + k_{\text{translocation}}^{ss} / k_{\text{peptide}}) \\ v_{ds} &= k_{\text{translocation}}^{ds} / (1 + k_{\text{translocation}}^{ds} / k_{\text{peptide}}) \end{aligned}$$

Here $v(F)$ is the overall translation rate under force F ; $f_{\text{open}}(F)$ is the probability that the junction is open at force F ; $v_{ds} = v(f_{\text{open}} = 0)$ is the rate of ribosome translation through a closed junction; $v_{ss} = v(f_{\text{open}} = 1)$ is the rate of ribosome translation through an open junction.

The probability that the junction is open, $f_{\text{open}}(F)$, depends on the number of base pairs opened per translocation step (here 3) and is quantified by the thermodynamic stability of the base pairs G_{bp} . This probability also depends on the effect of force applied to the ends of the hairpin, G_F , and on the destabilization of the junction induced by the ribosome, G_d . Since under our experimental condition the translocation step is rate-limiting for translation (see section 4 in supplementary discussion and Figure S7),

$$f_{open}(F) = 1 / (1 + \exp[(\Delta G_{bp} + \Delta G_F + \Delta G_d) / kT]) \quad (2)$$

We used mfold¹⁹ to calculate G_{bp} ; the values give good agreement with our experimental results on folding/unfolding RNA with optical tweezers (Figure S8). G_F is calculated using the wormlike-chain expression for force vs. extension²⁰. The parameters fit to the experimental results are G_d , v_{ss} , and v_{ds} . The 50% and 100% G•C sequence unwinding were fitted independently and yielded the same values of $G_d = 0.9$ kcal/mole per base pair, and $v_{ss} = 0.43$ or 0.44 codon/sec (Figure 2b and Table S2). The value of G_d so obtained is in the same range as determined for the T7 DNA helicase¹² and HIV-1 RT¹⁵. The best fit values of v_{ds} are 0.23 and 0.16 codon/sec for the unwinding of 50% and 100% G•C-containing hairpins, respectively.

Therefore, our data indicate that the ribosome uses two active mechanisms to promote junction unwinding: *open-state stabilization* (the role traditionally described for active helicases in the Betterton model, characterized by G_d), and *mechanical unwinding* (a new active mechanism in which the ribosome translocates by applying force to the closed state of the junction, characterized by v_{ds}). In the first mechanism, the ribosome binds and interacts preferentially with the open form of the junction, favoring this state in the thermal fluctuations (corresponding to increasing k_{open}/k_{closed} in Scheme 1), therefore increasing the probability for the ribosome to translocate unhindered. It has been shown for helicases that such interactions do not require an external energy source because it is a result of the affinity between the helicase and the junction²¹. No known nucleic acid helicase motifs are found in ribosomal proteins; however, a mutational study implicated several positively charged residues on ribosomal proteins S3 and S4 at the mRNA entry site in ribosome helicase activity, presumably by preferentially interacting with phosphate groups on the single-stranded mRNA backbone⁷. The identical value of G_d extracted from unwinding of the 50% and 100% G•C-containing hairpins indicate that the open-state stabilization mechanism in ribosomes has no significant base preference.

In the Betterton model, the ribosome can only translocate when encountering an open-state junction, whether occurring naturally or induced by the ribosome. However, when the ribosome encounters the junction in the closed state, the mechanical unwinding mechanism comes into play, allowing the ribosome to break open the junction and translocate forward. A translating ribosome can thus use part of the energy of GTP hydrolysis and peptide bond formation, coupled to its translocation, to apply force and rip the junction open. The force applied by the ribosome on the junction lowers the free energy barrier between the pre-translocation closed state and the post-translocation state, therefore opening this reaction path (labeled by $k_{translocation}^{ds}$ in Scheme 1). The smaller value of v_{ds} for unwinding 100% G•C than for unwinding 50% G•C indicates that increasing G•C content increases this barrier.

The molecular mechanism of ribosome translocation along mRNA is of intense current interest²². Cryo-EM studies of ribosome translocation intermediates stalled by a pseudoknot revealed a distorted conformation of the P-site tRNA, suggesting tension on the tRNA•mRNA linkage¹. Our results provide direct evidence that such tension could be used

to open the RNA junction. Thus, we postulate that inter- and intra-subunit ribosomal conformational changes associated with translocation²²⁻²⁷ generate a force that pulls on the tRNA•mRNA complex and promotes unwinding at the mRNA entry site (Figure 3). This tension may mediate ribosomal sensing of a high translocation barrier from a stable downstream mRNA structure, and give rise to the observed strong correlation between frameshifting efficiency and pseudoknot mechanical stability²⁸. Single-molecule studies²⁹ have found that the rupture force between a ribosome and an mRNA goes from essentially zero with no tRNAs bound to 15 pN with tRNAs in both the P- and A-sites; this high mechanical stability of the tRNA•mRNA linkage is needed to communicate mechanical tension to the base-paired hairpin at the mRNA entry site during translocation.

The unwinding mechanisms revealed in our studies serve as a quantitative basis for understanding how elongation rates are regulated by structured mRNAs. What are the physiological consequences of a second, active mechanism for the ribosomal helicase? First, the existence of a mechanism that uses translocation energy to disrupt the single-strand/double-strand junction insures a minimal basal rate of translation in the cell. It should also facilitate stripping off potential roadblocks to elongation such as mRNA-binding proteins, tRNAs, etc. Second, it means that no regular secondary structure represents an insurmountable barrier for the ribosome. Instead, specialized, mechanically-stable structures, such as pseudoknots¹ or combinations of such structures (hairpins and internal Shine-Dalgarno sequences²) are used to temporarily stall the ribosome, thus providing a mechanical basis for cellular regulation of elongation rates. The existence of this additional mechanical unwinding mechanism in ribosomes suggests that it may also be employed by other helicases, especially those with interdomain or intersubunit motions. The proposed unwinding model gives testable predictions for ribosomes bearing mutations in ribosomal proteins at the mRNA entry site or in proteins critical for translocation³⁰. Such studies will help elucidate the detailed underlying molecular interactions involved in ribosome function and in the two active unwinding mechanisms established here.

Methods

The materials, protocols, and experimental procedures have been described in our previous study⁸, except that an optical tweezers instrument with higher spatial resolution was used for this study. All data were obtained at 24.5-26.5 °C.

Translation steps in each trajectory were detected by algorithms written in Matlab. The pause times from all ribosomes under the same experimental condition were pooled together to calculate the average translation rate by a boot-strapping method: i) half of all pause times are randomly selected, histogrammed, and fitted to a single exponential; ii) this procedure is repeated for >1000 times; iii) the average translation rate and its error are determined as the average and the standard deviation/ 2 of the fitted rate constants from all the repeats. This procedure is very insensitive to the bin size used.

In Equation 2, The effect of force on the free energy of the open junction, G_F , is calculated from the worm-like chain model²⁰ for RNA single strands as $\Delta G_F = - \int_0^F x_{nt}(F') dF'$,

where $x_m(F')$ is the total extension of the single-strands released per translocation step under force F' .

Supplementary Material

Refer to Web version on PubMed Central for supplementary material.

Acknowledgments

We thank members of the Tinoco and Bustamante labs for helpful discussions, especially Dr. Steven B. Smith for his generous help with the optical tweezers, Dr. Jeffrey Moffitt for advice on data analysis, and Dr. Christian Kaiser for helpful suggestions. Our work was supported by grants from the National Institutes of Health (to I.T., C.B. and H.F.N.), and the Human Frontiers Science Program (to I.T. and H.F.N.).

References

- Giedroc DP, Cornish PV. Frameshifting RNA pseudoknots: Structure and mechanism. *Virus Res.* 2009; 139:193–208. [PubMed: 18621088]
- Tsuchihashi Z. Translational Frameshifting in the *Escherichia coli* dnaX Gene *in vitro*. *Nucleic Acids Research.* 1991; 19:2457–2462. [PubMed: 1710356]
- Nackley AG, et al. Human catechol-O-methyltransferase haplotypes modulate protein expression by altering mRNA secondary structure. *Science.* 2006; 314:1930–1933. [PubMed: 17185601]
- Duan JB, et al. Synonymous mutations in the human dopamine receptor D2 (DRD2) affect mRNA stability and synthesis of the receptor. *Human Molecular Genetics.* 2003; 12:205–216. [PubMed: 12554675]
- Young JC, Andrews DW. The signal recognition particle receptor alpha subunit assembles co-translationally on the endoplasmic reticulum membrane during an mRNA-encoded translation pause *in vitro*. *Embo Journal.* 1996; 15:172–181. [PubMed: 8598200]
- Watts JM, et al. Architecture and secondary structure of an entire HIV-1 RNA genome. *Nature.* 2009; 460:711–U787. [PubMed: 19661910]
- Takyar S, Hickerson RP, Noller HF. mRNA helicase activity of the ribosome. *Cell.* 2005; 120:49–58. [PubMed: 15652481]
- Wen JD, et al. Following translation by single ribosomes one codon at a time. *Nature.* 2008; 452:598–U592. [PubMed: 18327250]
- Yusupova GZ, Yusupov MM, Cate JHD, Noller HF. The path of messenger RNA through the ribosome. *Cell.* 2001; 106:233–241. [PubMed: 11511350]
- Keller D, Bustamante C. The mechanochemistry of molecular motors. *Biophys J.* 2000; 78:541–556. [PubMed: 10653770]
- Patel SS, Donmez I. Mechanisms of helicases. *J Biol Chem.* 2006; 281:18265–18268. [PubMed: 16670085]
- Johnson DS, Bai L, Smith BY, Patel SS, Wang MD. Single-molecule studies reveal dynamics of DNA unwinding by the ring-shaped T7 helicase. *Cell.* 2007; 129:1299–1309. [PubMed: 17604719]
- Lionnet T, Spiering MM, Benkovic SJ, Bensimon D, Croquette V. Real-time observation of bacteriophage T4 gp41 helicase reveals an unwinding mechanism. *Proc Natl Acad Sci U S A.* 2007; 104:19790–19795. [PubMed: 18077411]
- Manosas M, Xi XG, Bensimon D, Croquette V. Active and passive mechanisms of helicases. *Nucleic Acids Research.* 2010; 38:5518–5526. [PubMed: 20423906]
- Kim S, Schroeder CM, Xie XS. Single-Molecule Study of DNA Polymerization Activity of HIV-1 Reverse Transcriptase on DNA Templates. *J Mol Biol.* 2010; 395:995–1006. [PubMed: 19968999]
- Betterton MD, Julicher F. Opening of nucleic-acid double strands by helicases: Active versus passive opening. *Physical Review E.* 2005; 71:011904.

17. Tinoco I, Wen JD. Simulation and analysis of single-ribosome translation. *Physical Biology*. 2009; 6:025006. [PubMed: 19571367]
18. Rodnina MV, et al. GTPase mechanisms and functions of translation factors on the ribosome. *Biological Chemistry*. 2000; 381:377–387. [PubMed: 10937868]
19. Zuker M. Mfold web server for nucleic acid folding and hybridization prediction. *Nucleic Acids Research*. 2003; 31:3406–3415. [PubMed: 12824337]
20. Tinoco I, Bustamante C. The effect of force on thermodynamics and kinetics of single molecule reactions. *Biophysical Chemistry*. 2002; 101:513–533. [PubMed: 12488024]
21. Lohman TM, Tomko EJ, Wu CG. Non-hexameric DNA helicases and translocases: mechanisms and regulation. *Nat Rev Mol Cell Bio*. 2008; 9:391–401.10.1038/Nrm2394 [PubMed: 18414490]
22. Fischer N, Konevega AL, Wintermeyer W, Rodnina MV, Stark H. Ribosome dynamics and tRNA movement by time-resolved electron cryomicroscopy. *Nature*. 2010; 466:329–333. [PubMed: 20631791]
23. Moazed D, Noller HF. Intermediate States in the Movement of Transfer-RNA in the Ribosome. *Nature*. 1989; 342:142–148. [PubMed: 2682263]
24. Frank J, Agrawal RK. A ratchet-like inter-subunit reorganization of the ribosome during translocation. *Nature*. 2000; 406:318–322. [PubMed: 10917535]
25. Schuwirth BS, et al. Structures of the bacterial ribosome at 3.5 angstrom resolution. *Science*. 2005; 310:827–834. [PubMed: 16272117]
26. Valle M, et al. Locking and unlocking of ribosomal motions. *Cell*. 2003; 114:123–134. [PubMed: 12859903]
27. Peske F, Matassova NB, Savelsbergh A, Rodnina MV, Wintermeyer W. Conformationally restricted elongation factor G retains GTPase activity but is inactive in translocation on the ribosome. *Molecular Cell*. 2000; 6:501–505. [PubMed: 10983996]
28. Chen G, Chang KY, Chou MY, Bustamante C, Tinoco I. Triplex structures in an RNA pseudoknot enhance mechanical stability and increase efficiency of -1 ribosomal frameshifting. *Proc Natl Acad Sci U S A*. 2009; 106:12706–12711. [PubMed: 19628688]
29. Uemura S, et al. Peptide bond formation destabilizes Shine-Dalgarno interaction on the ribosome. *Nature*. 2007; 446:454–457. [PubMed: 17377584]
30. Cukras AR, Southworth DR, Brunelle JL, Culver GM, Green R. Ribosomal proteins S12 and S13 function as control elements for translocation of the mRNA : tRNA complex. *Molecular Cell*. 2003; 12:321–328. [PubMed: 14536072]

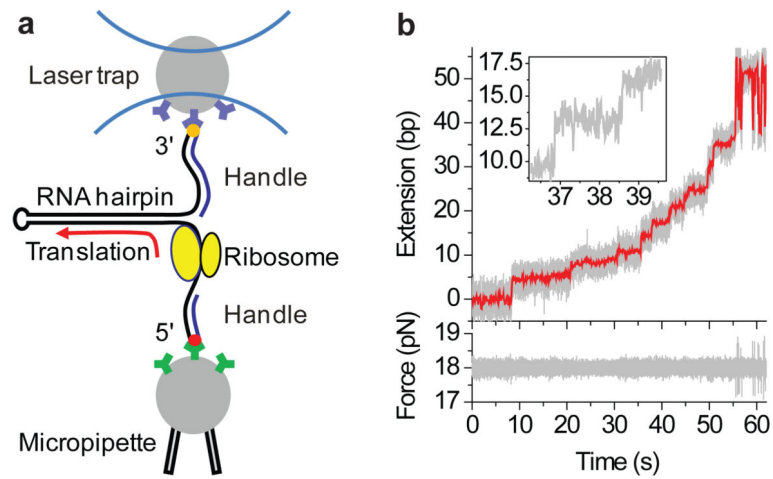


Figure 1.

Experimental setup. a, Schematic drawing showing the attachment of the ends of the mRNA hairpin to the two beads⁸. The mRNA sequences are shown in Figure S1. b, A trajectory for translation of hpVal_{GC50} mRNA under 18 pN force (gray: 1000 Hz; red: 10 Hz). Extension change is in units of number of base pairs (bp) opened. Hopping of the residual hairpin is observed at the end of the trajectory due to its instability under force. Inset: zoomed-in view of step-wise extension change for two steps (100 Hz).

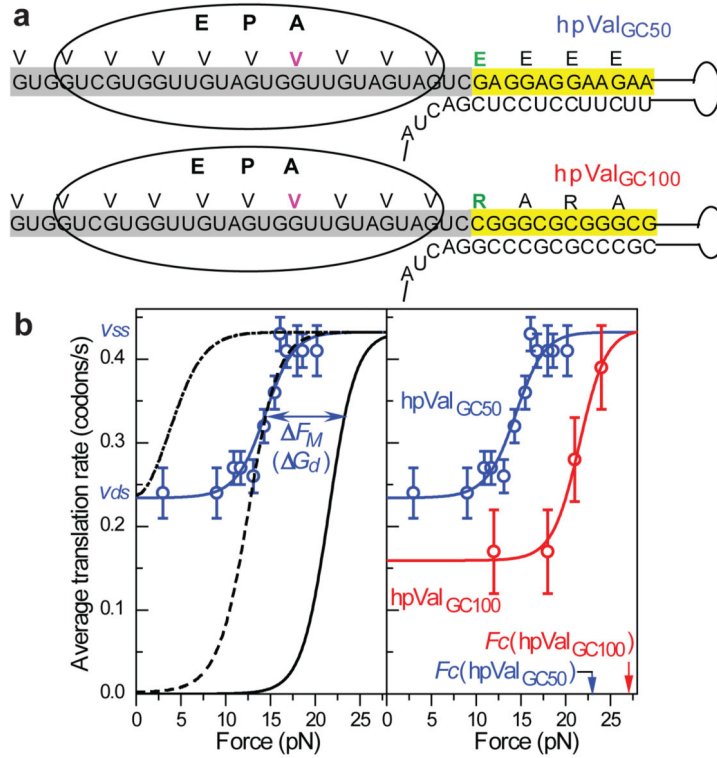


Figure 2.

Dependence of translation rate on force and mRNA G•C content. **a**, Schematic drawing showing that when the i^{th} codon in the A site (magenta) is translated, the subsequent translocation corresponds to unwinding the $(i+4)^{\text{th}}$ codon downstream (green) because the ribosome covers about 13 bases of single-stranded mRNA from its P site to the mRNA entry site. Only the sequence in the hairpin region is shown. **b**, Left panel: translation rate dependence on force for hpVal_{GC50} mRNA (~50% G•C unwinding). (i) *Blue circles*: experimental data. (ii) *Black solid, dashed, and dot-dashed lines*: predicted force dependence by the Betterton model, $v = v_{ss}f_{open}$, with $G_d = 0, 1.1,$ and 2.2 kcal/mole per bp, respectively. The three lines represent (*solid*) a totally passive helicase, (*dashed*) the best fit to F_M and the high-force plateau, and (*dot-dashed*) the best fit to the two plateaus, respectively. (iii) *Blue line*: best fit by Equation 1: $v = v_{ss}f_{open} + v_{ds}(1-f_{open})$. The three fitting parameters, v_{ss} , v_{ds} , and G_d , largely determine the high-force plateau, the low-force plateau, and F_M (the shift in F_M relative to a totally passive helicase), respectively. Right panel: Translation rate dependence on force for hpVal_{GC100} mRNA with 100% G•C unwinding (*red circles*) and the best fit by Equation 1 (*red line*). The data and best fit for hpVal_{GC50} mRNA (blue; from the left panel) is shown again for reference. The fitting results for both mRNAs are summarized in Table S1. $n = 39$ -120 ribosomes for hpVal_{GC50} and 16-29 ribosomes for hpVal_{GC100}, respectively, at each force. The error bars are the s.e.m.

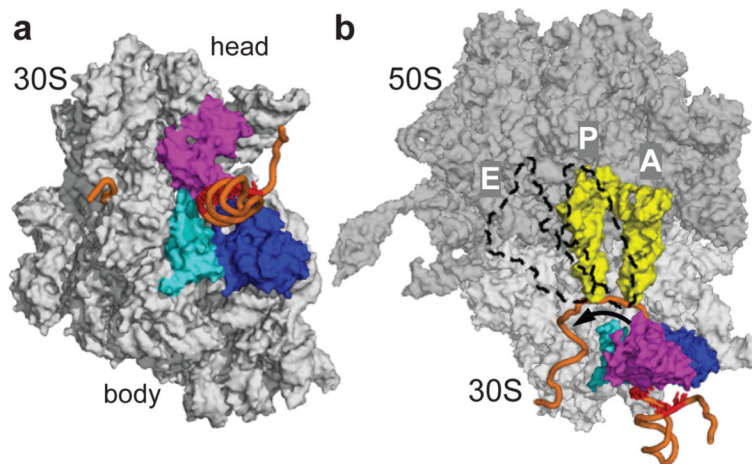
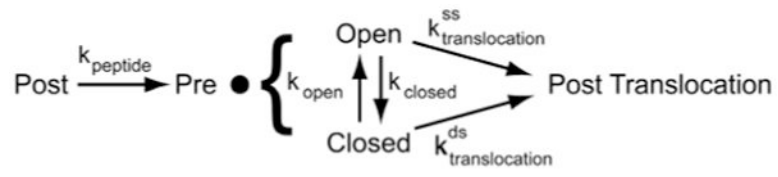


Figure 3.

The molecular arrangement of a translocating ribosome. a, The structure of the 30S subunit viewed from the mRNA entry site. About 30 nucleotides of single-stranded mRNA (orange) enter the ring-shaped mRNA entry site formed by the three colored ribosomal proteins, and wrap around the neck domain between the head and body. Secondary structures of the mRNA are excluded from the ribosome. b, Proposed ribosome unwinding mechanisms. The ribosome is rendered transparent so that the mRNA and the tRNAs inside can be clearly seen. Several base pairs (red) are destabilized by the ribosomal proteins at the entry site, which biases junction thermal fluctuations toward opening. Before translocation, the tRNAs (yellow) shift to the hybrid state (dashed). Then driven by ribosomal conformational changes, the tRNA anticodons translocate from the P and A sites on the 30S subunit to the E and P sites, and pull the mRNA along (black arrow). When encountering an open junction, translocation rectifies the junction opening events. Upon encountering a closed junction, the pulling force on the mRNA breaks open the mRNA junction at the entry site. The 50S and 30S subunits are from PDB files 2AW4 and 2AVY, respectively, and are modeled using PyMOL. The tRNAs and mRNA are for illustration purpose only.



Scheme 1.